PHYSICAL REVIEW B

CONDENSED MATTER

THIRD SERIES, VOLUME 43, NUMBER 10 PART B 1 APRIL 1991

Thermal expansion associated with the charge-density wave in $K_{0.3}MoO_3$

Matt R. Hauser, Brendan B. Plapp, and George Mozurkewich

Department of Physics, University of Illinois at Urbana–Champaign, 1110 West Green Street, Urbana, Illinois 61801

(Received 21 September 1990)

Thermal expansion was measured in two crystals of blue bronze ($K_{0.3}MoO_3$). At the Peierls temperature, the expansion coefficients exhibited a small steplike decrease along the chain direction, a nearly negligible change perpendicular to the cleavage planes, and a large steplike increase in the third, mutually orthogonal direction. Substantial departures from mean-field behavior were attributed to fluctuations, the width of the critical region was 8 K, and the temperature dependence was consistent with the three-dimensional XY model. The anisotropy of the steps was interpreted in terms of a transverse-optical periodic lattice distortion in an anharmonic lattice. Specimen length did not vary with electrical bias.

I. INTRODUCTION

Many quasi-one-dimensional metals undergo a second-order metal-insulator phase transition at a temperature T_P. The transition involves the formation of a periodic lattice distortion with an associated charge-density wave (CDW). Tremendous interest was generated by the observation in several of these materials of a form of collective electron transport involving the sliding of the CDW with respect to the crystal lattice.[1] However, many of the more traditional solid-state properties still lack detailed understanding. One such property involves minima in elastic moduli at T_P.[2–4] Whereas elastic properties and thermal expansion are interrelated thermodynamically, an investigation of thermal expansion should contribute to our overall understanding of basic CDW properties.

The modulus minima may be due to fluctuations. These materials are likely candidates to exhibit wide fluctuation regions near T_P because of their short coherence lengths[5] and small specific-heat signatures[6–8] at the phase transition. Indeed, x-ray experiments in blue bronze ($K_{0.3}MoO_3$) have observed critical exponents appropriate to the XY model over a rather wide range of 10° or more on either side of T_P,[5] and the wide critical region is in qualitative agreement with an estimate based on the Ginzburg criterion.[9] The observation of XY behavior in several physical quantities leads to definite predictions for the critical behavior of the thermal-expansion coeficient.[9]

Section II describes our experimental method and Sec. III presents results for blue bronze. Section IV analyzes the contribution of critical fluctuations to the expansion coefficients, and Sec. V relates them thermodynamically to previous investigations of specific heat and elastic moduli. In Sec. VI the results are interpreted in terms of an anharmonic lattice subjected to a transverse-optical periodic lattice distortion, and Sec. VII offers a reason for the transverse polarization of the distortion. Section VIII contains summary remarks.

II. EXPERIMENTAL METHOD

Expansion was measured on two crystals of blue bronze ($K_{0.3}MoO_3$). As blue bronze exhibits monoclinic symmetry, measurements in four directions are needed to determine the complete expansion tensor. The samples were shaped by grinding with Al_2O_3 powder such that, between them, five distinct crystallographic directions were accessible. These directions will be described by giving components of vectors spanning direct space [· · ·] or reciprocal space (· · ·), using the unit cell of Graham and Wadsley.[10]

Sample A, grown by Alavi at the University of California, Los Angeles, was prepared in the form of a rectangular parallelepiped with edge lengths of about 4 mm. One pair of faces was accurately defined by the $(20\bar{1})$ cleavage planes. Using Laue photography, a second pair was oriented normal to the chain direction [010] with an accuracy of 1°. The final pair was oriented normal to [102], orthogonal to the other faces. Sample B, grown by Lyons and Ramli at the University of Illinois, was prepared in the form of a hexagonal prism with length about 12 mm along its axis and about 4 mm between the other pairs of faces. The prism axis was along the chain direction; the (010) faces were oriented within 1° by Laue photography. The cleavage planes defined $(20\bar{1})$ faces, and the final pairs of faces were prepared within 2° of the (100) and (001) growth facets.

Expansion of the samples was measured with a capacitive dilatometer based on the design of Steinitz *et al.*[11] The samples were held between vitreous silica plates for electrical insulation from the copper probe. Capacitance was measured at 415 Hz using a coaxial bridge[12] based on a seven-decade ratio transformer. Thermal expansion measurements were made in a vacuum during slow temperature sweeps with heating stepped under computer control. The bridge was balanced at the beginning of each run, and the imbalance signal was converted into capacitance and then into specimen length. The thermal-expansion coefficient was calculated by taking a numeri-

cal derivative of the sample length. Performance was checked using test specimens of vitreous silica, obtaining agreement to ±1 ppm/K with compiled data on silica and oxygen-free-high-conductivity (OFHC) copper.[13]

Most thermal-expansion measurements were taken with increasing temperature. To check that temperature gradients throughout the apparatus were negligible, some measurements were taken with decreasing temperature. Agreement between upward and downward sweeps was obtained using sweep rates not exceeding 4° per h. The transition temperature T_P of sample A was determined by the peak in the resistance derivative-$d(\ln R)/dT$. To measure resistance along the direction of highest conductivity, the faces perpendicular to [010] were electroplated with copper electrodes. Because of the small resistance of the large cross-section specimen, its resistance was measured in a pseudo-four-probe configuration, using separate current and voltage leads.

Measurements of length versus electric field were taken with the sample and dilatometer entirely immersed in liquid nitrogen. A current was passed through the specimen along the [010] direction using one pair of leads, and the voltage was measured using the other pair. The heaters were not used, and the only temperature variation was due to Ohmic heating in the sample.

III. RESULTS

Figure 1 shows thermal expansion coefficients along the [102] and (20$\bar{1}$) directions in sample A. The sharp minimum in α along [102] occurred at 179.4±0.1 K, while the peak in the resistance derivative occurred at 179.6±0.4 K. Figure 2 shows thermal-expansion coefficients along (010), (100), (001), and (20$\bar{1}$) in sample B. The electrical resistance of sample B was not measured, but T_P appears to be a few degrees higher than in sample A.

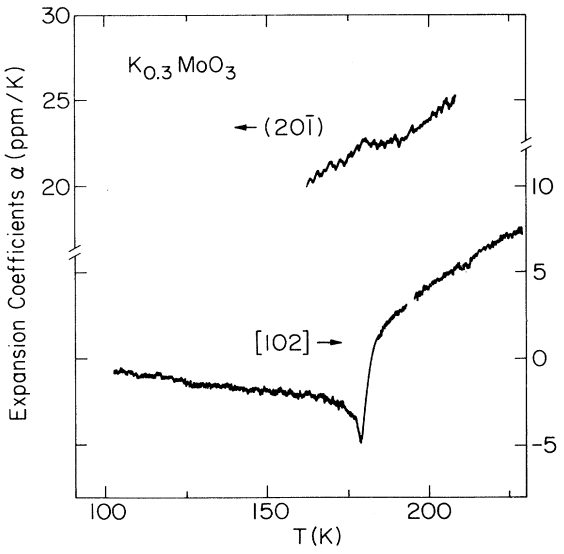

FIG. 1. Thermal expansion coefficients of sample A.

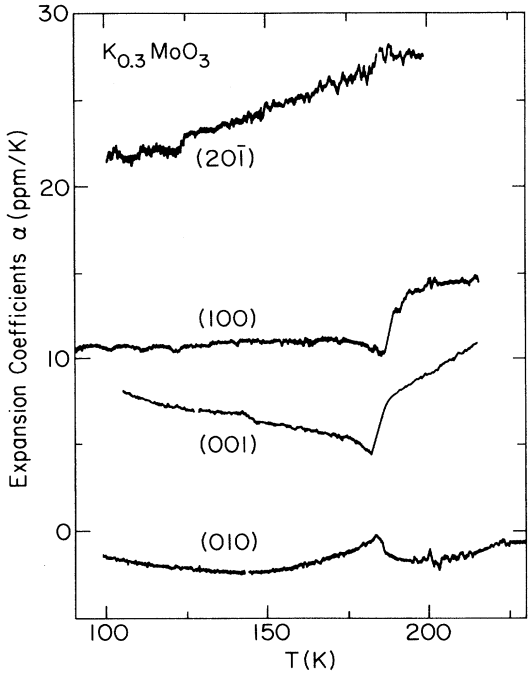

FIG. 2. Thermal expansion coefficients of sample B.

The data along [102], (001), and (100) show a sudden increase at T_P, largest along [102]. In the mean-field theory one expects a simple discontinuity ("step") at T_P. Instead we find a precursor dip which indicates the importance of fluctuations. Along (010) we find a step decrease with precursor peak. Along (20$\bar{1}$), sample A shows a very small decrease while sample B shows no effect. The precursor is sharper in sample A, which we therefore believe is a higher-quality crystal.

Apart from the behavior near T_P, these results are in general agreement with the x-ray measurements of Ghedira *et al.*[14] The expansion is largest perpendicular to the cleavage planes and is smallest (nearly zero) along the chain direction. The magnitudes of the various coefficients are similar, although not identical, to values deduced from the x-ray work. These measurements show no evidence for an incommensurate-to-commensurate (lock-in) transition.

Elastic moduli of some quasi-one-dimensional CDW compounds are known to vary when the CDW slides.[15,16] No such effect has been observed in blue bronze,[3,4] at least not at 77 K.[17] Nevertheless, we investigated whether the length might depend on sliding. Measurements were made at 77 K in sample A along all three directions. To an accuracy of ±1 ppm, we found no effect which could not be attributed to Joule heating.

IV. FLUCTUATIONS

The temperature dependence of the expansion coefficient does not show the simple step classically associated with second-order transitions. The precursor dip (or peak, for data along the chain direction) signifies a

contribution from fluctuations. In the regime of Gaussian fluctuations, the thermal expansion may be represented by

$$\alpha(T)=\begin{cases}\sum_{n=0}^{3} a_n T^n-\dfrac{G}{(T-T_P)^{1/2}}, & T>T_P\ ,\\ \sum_{n=0}^{3} a_n T^n-\dfrac{\sqrt{2}G}{(T_P-T)^{1/2}}+H, & T<T_P\end{cases}\ . \tag{1}$$

The polynomial sum represents a smooth background variation, H is the magnitude of the mean-field step, and G is the strength of the Gaussian term, whose form assumes three-dimensional fluctuations.

The regime of validity of Gaussian fluctuations was found as follows. Treating $\{a_n\}$, G, and H as adjustable parameters, Eq. (1) was fit to $\alpha(T)$ excluding data for which $|T-T_P|<T^*$. The fit was repeated for various values of T^*, and Fig. 3 presents the corresponding variation with T^* of G and of σ^2, the mean-square deviation per degree of freedom (variance). For $T^*>8$ K, σ^2 is essentially constant. For smaller T^*, σ^2 increases rapidly, indicating failure of the Gaussian representation. The figure also shows σ^2 calculated while holding $G=0$, indicating failure of the mean-field form within 17 K of T_P. Correspondingly, G behaves rather erratically for $T^*>17$ K, then attains a fairly well-defined value for $T^*\approx 10$ K. For $T^*<8$ K, G decreases because the data no longer diverge as fast as the Gaussian prediction. Therefore, we experimentally identify the width of the critical region to be $\Delta T=8$ K.

The width of the regime in which fluctuations are important (± 17 K) agrees with a recent analysis of the specific heat.[18] Moreover, the width of the regime of *critical* fluctuations (± 8 K) agrees with recent x-ray investigations by Girault *et al.*[5] Their diffraction experiments measured order parameter, correlation length, and susceptibility as functions of reduced temperature $t=|(T/T_P)-1|$, finding critical exponents in good agreement with the XY model ($n=2$) in three dimensions ($d=3$) over a critical region ≈ 10 K. The expectation of a wide critical region has been challenged by Chandra,[19] who calculated a very small width by using a one-dimensional Ginzburg-Landau Hamiltonian appropriate to a single chain. In the absence of long-range interactions, fluctuations suppress the phase transition in that model to $T=0$. Thus, a correct treatment of the observed transition at T_P requires attention to the interchain couplings. The parameters of the real three-dimensional system have not yet been determined. However, by using experimental correlation lengths and experimental specific heats appropriate to the real three-dimensional transition at T_P, Aronovitz *et al.*[9] deduced a width of the critical region consistent with the x-ray experiments and with the present result.

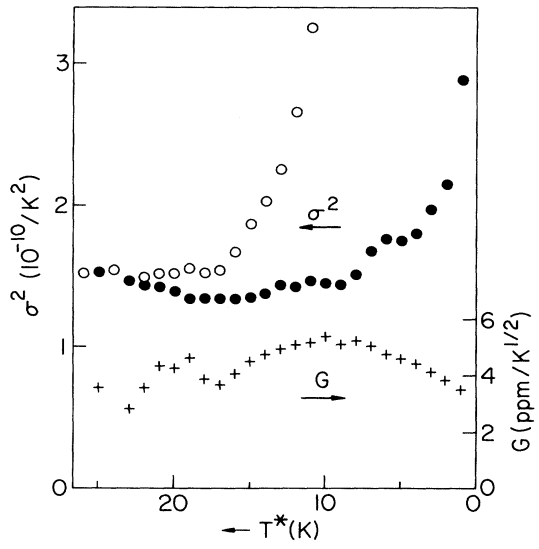

FIG. 3. Deduction of regime of validity of Gaussian fluctuations, using expansion data from sample A along [102]. Points within T^* degrees of T_P were excluded from the fit. Solid circles: σ^2 with G variable. Crosses: corresponding values of G. Open circles: σ^2 with constraint $G=0$.

On general thermodynamic grounds, the thermal expansion coefficients (as well as elastic compliances) should show the same behavior as the specific heat. The $n=2$, $d=3$ prediction for the specific-heat exponent is $\alpha=-0.008$; this small, negative value means that the specific heat, expansion coefficients, and compliances should show an extremely sharp cusp. However, Aronovitz *et al.*[9] argued that such a sharp cusp would be overwhelmed in the experimentally accessible temperature range by a weaker cusp, $t^{-\alpha+\omega\nu}$, derived as a correction to scaling. For $n=2$ and $d=3$, $-\alpha+\omega\nu=0.53$.

The practical difficulty with fitting such a cusp to data is that the form can only hold over a limited temperature range near T_P. Farther from T_P it is guaranteed to fail, because, unlike the classical behavior, it continues to increase without bound. This difficulty has recently been obviated by Chen and co-workers who have formulated a theoretically consistent interpolation between the classical and critical regimes.[20] We have adapted that formulation[21] to thermal expansion by replacing $T\partial^2(\Delta A^*)/\partial T^2$, which gives the specific heat, by $T_P\partial^2(\Delta A^*)/\partial T\partial\sigma_i$, where $\Delta A^*$is the critical contribution to the free energy and σ_i is a stress component. Then we assume that derivatives for T and σ_i are proportional through $dT_P/d\sigma_i$, the sensitivity of the transition temperature to stress. Additional fitting parameters are $\bar{u}$ and $\eta\equiv\Lambda/c_t^{1/2}$ (which determine the shape of the anomaly and are defined in Ref. 21), the transition temperature T_{P0}, and the coefficients of a cubic polynomial representing a smooth background variation. Further details of the fitting procedure are planned to be given elsewhere.[22]

Acceptable fits are obtained with $\bar{u}=2.6\pm0.1$, $\eta=0.6\pm0.1$, and $T_{P0}=180.58\pm0.02$ K. The dashed line in Fig. 4 shows our best fit to the three-dimensional XY model. The fit is distinctly narrower than the data. The solid line includes an artificial broadening of about 2°, which might represent an inherent sample inhomogeneity. Because of the need to introduce a broadening, we cannot state without reservation that the XY prediction is obeyed. Nevertheless, these data are consistent with the

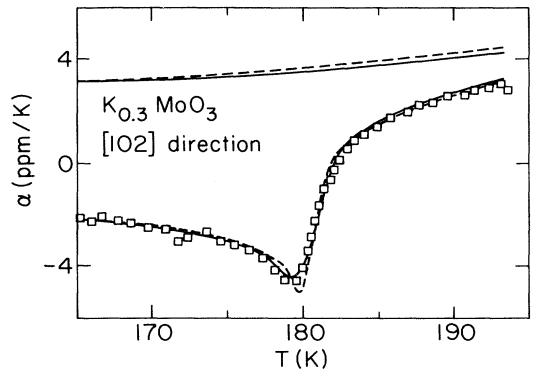

FIG. 4. Symbols: data from sample A (80% of points omitted for clarity). Dashed line: best fit to three-dimensional XY model. Solid line: best fit after including 2 K broadening. Corresponding polynomial backgrounds are also shown.

XY model.

For an ideal sample, the minimum in α occurs exactly at T_P. For our samples, the value of T_{P0}, that gives the best fit does not coincide with the minimum in α. This is an indication of an inhomogeneous T_P. Recalling the asymmetric shape of the ideal $\alpha(T)$, it is easy to show that a symmetric distribution of T_P around a central T_{P0} will cause the minimum of the measured α to occur below T_{P0}. The magnitude of the separation between the fitted T_{P0} and the minimum may be used as a quantitative measure of inhomogeneity.

V. THERMODYNAMICS

The fit described in the previous section enables us to extract the magnitude of the mean-field step, which we define as the difference between the low-temperature data and the fitted background. The resulting number is unbiased, in the sense that we do not need to guess a background "by eye", and we consider it to be reliable because it is only moderately sensitive to whether an artificial broadening was introduced. Table I compiles the results.

The tensor of expansion-coefficient steps was determined by least squares,[23] using all seven table entries to determine the four tensor components. To simplify the notation, we define an orthogonal coordinate system with x along $(20\bar{1})$, y along (010), and z along [102]. The nonzero components are

$$\Delta\alpha_{xx} = -0.2 \pm 0.7 \text{ ppm/K} ,$$

$$\Delta\alpha_{yy} = -1.4 \pm 0.2 \text{ ppm/K} ,$$

$$\Delta\alpha_{zz} = +4.3 \pm 0.7 \text{ ppm/K} ,$$

and

$$\Delta\alpha_{xz} = \Delta\alpha_{zx} = +0.5 \pm 0.8 \text{ ppm/K} .$$

The large uncertainties are primarily due to a variation between the specimens.

The magnitudes of the mean-field steps should obey the Ehrenfest relations for second-order phase transitions.[24] As generalized to anisotropic materials,[25] these relations are

$$-dT_P/d\sigma_i = \Delta\alpha_i T_P/\Delta C_\sigma , \tag{2a}$$

$$-dT_P/d\sigma_i = \Delta S_{ii}/\Delta\alpha_i , \tag{2b}$$

where σ_i and α_i are components of stress and expansion tensors expressed in Voigt notation, C_σ is the specific heat at constant stress, and S_{ii} are isothermal elastic compliances. The Δ denotes the difference between the quantity above and below T_P. The pressure dependence of the transition temperature has been measured by Wang *et al.*,[26] and by Mihaly and Canfield,[27] from which we adopt an average value

$$dT_P/dP = -\sum_i dT_P/d\sigma_i = -1.25 \pm 0.15 \text{ K/kbar} .$$

From Eq. (2a),

$$\Delta C_\sigma = T_P\left(\sum_i \Delta\alpha_i\right)/(dT_P/dP)$$

$$= -1.4 \pm 0.5 \text{ J (mol formula unit)}^{-1}\text{K}^{-1} .$$

This result can be compared with three experimental determinations. Our fit of Johnston's specific-heat measurement[7] to the XY model gives -1.8 J/mol K, Komaten[6] extracted a step of -2 J/mol K, and Kwok and Brown[8] quoted a step of -3.6 J/mol K.

The isothermal compliance steps could be determined from Eq. (2b) except that the sensitivities of T_P to the stress components are not individually known. Instead, we equate the right-hand sides and use the value of ΔC_P that satisfies Eq. (2a) to deduce compliance steps

$$\Delta S_{xx} = -(0.01 \pm 0.05) \times 10^{-14} \text{ m}^2/\text{N} ,$$

$$\Delta S_{yy} = -(0.9 \pm 0.4) \times 10^{-14} \text{ m}^2/\text{N} ,$$

and

$$\Delta S_{zz} = -(8 \pm 3) \times 10^{-14} \text{ m}^2/\text{N} .$$

Young's modulus Y_i along a given direction is the reciprocal of the corresponding diagonal compliance. Steps in Young's modulus have been measured at audio frequencies by the vibrating-plate technique (presumably

TABLE I. Magnitudes of expansion-coefficent steps $\Delta\alpha_i$ at T_P. Note: Estimated uncertainties ±0.2 ppm/K.

Direction	Sample	Magnitude (ppm/K)
(010)	*A*	−1.3
	B	−1.5
$(20\bar{1})$	*A*	−0.3
	B	0
[102]	*A*	+4.9
(100)	*B*	+2.9
(001)	*B*	+2.4

isothermally) by Bourne and Zettl,[3] with results corresponding to

$$\Delta S_{yy} = -(1.4 \pm 0.6) \times 10^{-14} \text{ m}^2/\text{N}$$

and

$$\Delta S_{zz} = -(32 \pm 10) \times 10^{-14} \text{ m}^2/\text{N} .$$

The *yy* component is consistent, but the *zz* component is a few times larger than the value we expect. Although ratios may be expected to be more reliable than absolute measurements, their ratio of compliance steps differs substantially from our ratio of squares of $\Delta\alpha_i$, even after taking account of the substantial error bars on each.

Saint-Paul and Tessema[4] have measured longitudinal sound velocities and corresponding stiffnesses at radio frequencies. Those measurements were adiabatic, not isothermal. Furthermore, in order to convert to compliances, it is necessary to invert the entire stiffness matrix, most of whose 13 elements are unknown. If we nevertheless take $\Delta S_{ii} = -\Delta C_{ii}/C_{ii}^2$, we obtain $\Delta S_{xx} = 0$,

$$\Delta S_{yy} = -0.9 \times 10^{-14} \text{ m}^2/\text{N} ,$$

and

$$\Delta S_{zz} = -1.5 \times 10^{-14} \text{ m}^2/\text{N} .$$

The first two values agree with our expectations, while the last is smaller by a factor of 5. It is possible that measurements of the full compliance matrix, combined with conversions from adiabatic to isothermal moduli, would resolve the discrepancy.

VI. ANHARMONIC MODEL

The anisotropy of the thermal expansion coefficients can be understood in terms of the nature of the periodic lattice distortion (PLD) associated with the CDW in blue bronze. The distortion, as determined for the molybdenum ions by Sato *et al.*[28] using x-ray diffraction, exhibits these main features: The displacements of the Mo(3) ions are principally along [102], with smaller components along $(20\bar{1})$ and [010]. The much smaller Mo(2) and Mo(1) displacements are roughly along (100) and [102], respectively. The entire displacement pattern is modulated with wave vector $\mathbf{Q} = (1, q_b, -0.5)$, where $q_b \approx 0.75$, but is incommensurate with the parent structure. The $(1,0,-0.5)$ component of $\mathbf{Q}$ causes the displacement pattern to have opposite sign on alternate $(20\bar{1})$ planes, possibly due to interplane Coulomb interactions, but this detail will not concern us here. This PLD may be described as a frozen transverse-optical phonon.

Consider the expansion along [102]. The Mo lattice along [102] will be treated like a string of balls and springs. Whereas the Mo(3) and Mo(2) ions have different distortion amplitudes, the PLD causes the springs to have different lengths. Therefore, for the purpose of understanding the essential physics, the PLD will be modeled by a dimerized one-dimensional chain, with springs of alternating lengths $l_0 \pm a$.

For small departures x from their undimerized lengths, the springs' total potential energy may generally be represented by

$$U_s(x) = N(e_s x + \tfrac{1}{2} f_s x^2 + \tfrac{1}{6} g_s x^3 + \tfrac{1}{24} h_s x^4) , \tag{3}$$

where $e_s = 0$ without loss of generality, and $g_s < 0$. Equilibrium, defined by $dU/dx = 0$, requires $x = 0$, for which the total length of the chain is Nl_0. After dimerization

$$U_d(x) = (N/2)[U_s(x+a) + U_s(x-a)] ,$$

provided that the value of a is constrained from fluctuating. (This amounts to mean-field theory.) Thus, $U_d(x)$ has the same form as $U_s(x)$ with the substitutions

$$\begin{aligned} e_d &= e_s + \tfrac{1}{2} g_s a^2 = \tfrac{1}{2} g_s a^2 , \\ f_d &= f_s + \tfrac{1}{2} h_s a^2 , \\ g_d &= g_s = g , \\ h_d &= h_s = h . \end{aligned} \tag{4}$$

Applying the equilibrium condition to U_d shows that the average lattice constant in the dimerized chain is longer by

$$\delta l = -\frac{\frac{1}{2} g a^2}{f_s + \frac{1}{2} h a^2} \approx \frac{g a^2}{2 f_s} . \tag{5}$$

The thermal expansion of a one-dimensional chain with the interaction potential given by Eq. (3) has been described in detail by Leibfried and Ludwig.[29] Its lattice constant is

$$l(T) = \tilde{l} - (g/2 f_s^2)\varepsilon , \tag{6}$$

where ε is the mean thermal energy per mode in the harmonic approximation. Making the classical approximation for T near T_P, $\varepsilon = k_B T$, results in a linear $l(T)$. $\tilde{l}$ is the $T = 0$ intercept of $l(T)$. [This differs from the zero-temperature lattice constant $l(T=0)$ due to zero-point fluctuations.] Thus, the thermal-expansion coefficient along the undimerized chain is

$$\alpha_s = -\frac{k_B g}{2 f_s^2 l_0} . \tag{7}$$

The dimerized chain expands more slowly. This is apparent upon inserting f_d for f_s and $\tilde{l} + \delta l$ for $\tilde{l}$ in Eq. (6). For temperatures far enough below T_P that a becomes constant,

$$\alpha_d = -\frac{k_B g}{2(f_s + \frac{1}{2} h a^2)^2 l_0} , \tag{8}$$

while in the vicinity of T_P, the temperature dependence of a must be taken into account. Recalling that a is proportional to the order parameter, its mean-field dependence is $a^2 = a_0^2 (T_P - T)/T_P$ for $T < T_P$ and $a^2 = 0$ for $T > T_P$. Thus, α undergoes a finite discontinuity at T_P of magnitude

$$\Delta\alpha = -\frac{g a_0^2}{2 f_s l_0 T_P} \tag{9}$$

to lowest order in the anharmonicity. However, if mean-field theory is not obeyed, α will have a more interesting behavior near T_P.

While the discussion so far has been for a one-dimensional chain, the three-dimensionality of the specimen allows dimerization along one direction to affect the expansion in other directions. Consider the two-dimensional lattice shown in Fig. 5. Dimerization along the horizontal direction without changing the vertical lattice constant causes all the vertical springs to elongate. The lattice will reduce its energy by shrinking vertically. Thus, the thermal-expansion effect associated with the dimerization along [102] should be expected to induce an opposite effect along (010).

To conclude this section, we give a crude estimate of the amplitude of the PLD. Because of the extreme approximations required to apply the simple balls-and-springs model to the complicated blue bronze structure, this estimate is valuable only to indicate that the order of magnitude is reasonable. The distortion amplitude may be obtained from the expansion step along [102] by Eq. (9) if g is estimated from the background expansion, Eq. (7):

$$a_0^2 = \left[\frac{k_B T_P}{f_s}\right]\frac{\Delta\alpha}{\alpha_s} . \tag{10}$$

The spring constant may be estimated as $f = Mv^2/l_0^2$ from the elementary treatment of the harmonic chain, where $v = 3.1\times10^5$ cm/s is the longitudinal velocity of sound along [102].[4] The basic, five-octahedra structural unit corresponds to a full dimerization repeat distance, whose length along [102] is[14] $2l_0 = 9.84$ Å and whose mass is that of 5 $K_{0.3}MoO_3$, i.e., $2M = 6.5\times10^{-22}$ g. Thus, $a_0 \approx 0.1$ Å, which is about twice the observed displacement of Mo(3).[28]

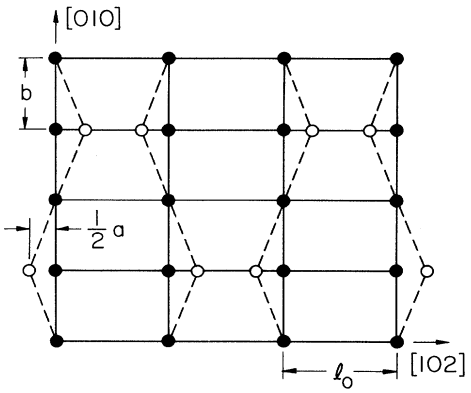

FIG. 5. Two-dimensional balls-and-springs model in high-temperature (solid lines, solid circles) and distorted (dashed lines, open circles) phases, illustrating the origin of the inverted expansion step along [010]. Distortion wavelength along [010] equals $4b$.

VII. WHY THE POLARIZATION IS TRANSVERSE

The transverse polarization of the CDW in blue bronze is a fact which still requires explanation. The Peierls argument is often illustrated with a longitudinal acoustic distortion. From a more general standpoint, the phenomenon can be viewed as an extended Jahn-Teller transition, in which a general symmetry reduction lowers the energies of some of the states involved.[30] Two specific examples, both applicable to molecular chains, have been analyzed in the literature. Both involve a modulation of the molecular bonding strength, resulting in either a longitudinal-optical distortion[31] or a transverse-optical one.[32] All these examples consider only a single quasi-one-dimensional band crossing the Fermi level.

Pouget *et al.*[33] proposed that the CDW in blue bronze simultaneously gaps two bands. A tight-binding band calculation by Whangbo and Schneemeyer[34] is beautifully consistent with this proposal. Among its strengths is the presence of an empty band just above the Fermi level, which can account for the previously unexplained[33] temperature dependence of the CDW wave vector.[35]

Simultaneous gapping of two bands requires not only a lattice distortion with the right wave vector but also a matrix element capable of scattering forward-going electrons on one band into backward-going electrons on the other band. Here we suggest that the most efficient way to provide the interband scattering is by modulating the distance between the chains on which the two bands are based. Both Mo(3) and Mo(2) orbitals[36] are involved in the bands which cross the Fermi level. However, according to the band calculation, the lower band has stronger

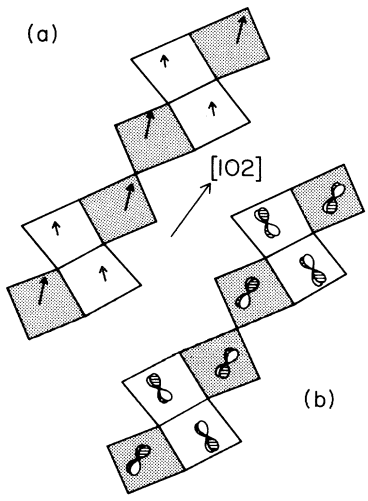

FIG. 6. Comparison of (a) the observed distortion pattern (Ref. 28) and (b) the orbitals from which the relevant bands are built (Ref. 34). Mo(3) chains are shaded, Mo(2) chains are unshaded. The chain direction is normal to the figure. (Adapted with permission of the American Chemical Society and of IOP Publishing Ltd.)

Mo(3) character while the higher is more strongly based on Mo(2). Therefore, it is productive to think of the bands as being built principally from one or the other of two types of chains: one chain based on a pair of corner-sharing octahedra containing Mo(3) sites, the other on a pair of edge-sharing octahedra containing Mo(2) sites. Scattering between the bands based on the two distinct chains is accomplished by the observed distortion pattern [Fig. 6(a)] which modulates the distance between these two types of chains, but not the distance between atoms within a chain. Furthermore, the orbitals upon which the lowest two bands are based [Fig. 6(b)] are oriented in such a way that the observed distortions efficiently (and presumably optimally) modify the relevant transverse hopping integrals.

VIII. SUMMARY

CDW formation in blue bronze introduces steps into the thermal-expansion coefficients at the CDW formation temperature T_P. In form, the steps are not simple discontinuities, as predicted by mean-field theory; they show precursor effects caused by fluctuations. The shapes are not precisely what is expected for the XY model in three dimensions, but the shapes are consistent with XY in three dimensions if sample inhomogenity is taken into account.

By introducing a transverse-optical lattice distortion into an anharmonic lattice, the anisotropy of the expansion coefficients is readily interpreted. A dimerized, anharmonic chain is longer than the corresponding undimerized chain but expands less quickly as temperature increases. This accounts for the upward step parallel to the displacement vector of the lattice distortion. Because of transverse coupling, the expansion effect along the dimerization direction is accompanied by an effect of opposite sign along the chain direction. Therefore, a downward step is observed along the chain direction. The same anharmonicity is thermodynamically related to the minima in various elastic moduli near T_P.

While the transverse polarization of the PLD in blue bronze has been known for several years, this is, to our knowledge, the first time that measurements other than diffraction have been interpreted in terms of the transverse distortion. We attribute the origin of the transverse distortion to the necessity of simultaneously gapping two bands, both of which cross the Fermi level. A transverse distortion is not the only way to accomplish this, but it seems to be an efficient way. Whereas the transition-metal trichalcogenides also have pairs of bands crossing the Fermi level, we speculate that their PLD's also are transversely polarized, and that their anharmonicities account for the observed minima in their moduli.

We discerned no dependence of specimen length on electric field. Perhaps this is not very surprising because the elastic moduli of blue bronze also are not modified when the CDW slides. It would be interesting to learn whether specimen length is bias-dependent in those compounds whose moduli soften in the sliding state.

ACKNOWLEDGMENTS

We have benefited enormously from discussions with Lee Link, Joseph Aronovitz, Paul Goldbart, Z. Y. Chen, and Richard Martin. David Johnston graciously provided unpublished data. This work was supported by the National Science Foundation Grant No. DMR-84-51935, with additional support from IBM.

[1]For reviews, see P. Monceau, in *Electronic Properties of Inorganic Quasi-One-Dimensional Compounds,* edited by P. Monceau (Reidel, Dordrecht, 1985), Vol. 2, p. 139; G. Grüner, Rev. Mod. Phys. **60**, 1129 (1988).

[2]J. W. Brill, Solid State Commun. **41**, 925 (1982).

[3]L. C. Bourne and A. Zettl, Solid State Commun. **60**, 789 (1986).

[4]M. Saint-Paul and G. X. Tessema, Phys. Rev. B **39**, 8736 (1989).

[5]S. Girault, A. H. Moudden, and J. P. Pouget, Phys. Rev. B **39**, 4430 (1989).

[6]K. Konate, thèse 3ème cycle, L'Université Scientifique et Medicale de Grenoble, 1984 (unpublished).

[7]D. C. Johnston (unpublished).

[8]R. S. Kwok and S. E. Brown, Phys. Rev. Lett. **63**, 895 (1989).

[9]J. A. Aronovitz, P. Goldbart, and G. Mozurkewich, Phys. Rev. Lett. **64**, 2799 (1990).

[10]J. Graham and A. D. Wadsley, Acta Crysallogr. **20**, 93 (1966).

[11]M. O. Steinitz, J. Genossar, W. Schnepf, and D. A. Tindall, Rev. Sci. Instrum. **57**, 297 (1986).

[12]B. P. Kibble and G. H. Rayner, *Coaxial AC Bridges* (Hilger, Bristol, 1984).

[13]*Thermophysical Properties of Matter,* edited by Y. S. Touloukian and C. Y. Ho (IFI-Plenum, New York, 1975), Vols. 12 and 13.

[14]M. Ghedira, J. Chenavas, M. Marezio, and J. Marcus, J. Solid State Chem. **57**, 300 (9185).

[15]J. W. Brill and W. Roark, Phys. Rev. Lett. **53**, 846 (1984); J. W. Brill, W. Roark, and G. Minton, Phys. Rev. B **33**, 6831 (1986).

[16]G. Mozurkewich, P. M. Chaikin, W. G. Clark, and G. Grüner, in *Charge-Density Waves in Solids,* edited by Gy. Hutiray and J. Sólyom (Springer, New York, 1985), p. 353; Solid State Commun. **56**, 421 (1985).

[17]A. Zettl, L. C. Bourne, J. Clarke, M. F. Crommie, M. F. Hundley, R. E. Thompson, and U. Walter, Synth. Met. **29**, F445 (1989).

[18]R. S. Kwok, G. Grüner, and S. E. Brown, Phys. Rev. Lett. **65**, 365 (1990).

[19]P. Chandra, J. Phys: Condens. Matter **1**, 3709 (1989); **1**, 10067 (1989).

[20]Z. Y. Chen, P. C. Albright, and J. V. Sengers, Phys. Rev. A **41**, 3161 (1990); Z. Y. Chen, A. Abbaci, S. Tang, and J. V. Sengers, Phys. Rev. A **42**, 4470 (1990).

[21]Z. Y. Chen, Phys Rev. B **41**, 9516 (1990).

[22]G. Mozurkewich and R. L. Jacobsen (unpublished).

[23]J. F. Nye, *Physical Properties of Crystals* (Oxford University, New York, 1985), Chap. 9.

[24]P. Ehrenfest, Leiden Comm. Suppl. **75b**, 8 (1933).

[25]L. R. Testardi, Phys. Rev. B **12**, 3849 (1975).

[26]X. Wang, L. Lu, H. Duan, B. J. Jin, and D. Zhang, Solid State

Commun. **69**, 127 (1989).
[27] G. Mihály and P. Canfield, Phys. Rev. Lett. **64**, 459 (1990).
[28]M. Sato, H. Fujishita, S. Sato, and S. Hoshino, J. Phys. C **18**, 2603 (1985).
[29]G. Leibfried and W. Ludwig, in *Solid State Physics,* edited by F. Seitz and D. Turnbull (Acdemic, New York, 1961), Vol. 12, p. 275 and especially pp. 336–339.
[30]R. E. Peierls, *Quantum Theory of Solids* (Clarendon, Oxford, 1955), Sec. 5.3.
[31]D. Baeriswyl and A. R. Bishop, J. Phys. C **21**, 339 (1988).
[32]D. Feinberg and J. Ranninger, J. Phys. C **16**, 1875 (1983).
[33]J. P. Pouget, C. Noguerra, A. H. Moudden, and R. Moret, J. Phys. (Paris) **46**, 1731 (1985).
[34]M. H. Whangbo and L. F. Schneemeyer, Ignorg. Chem. **25**, 2424 (1986).
[35]The temperature dependence cannot be attributed to a commensurate-incommensurate transition. No signature of the purported transition has been found in specific heat (Ref. 8), thermal expansion (this work), or elastic moduli (Ref. 4). Furthermore, diffraction measurements show only a gradual variation with temperature (Ref. 28), and in doped samples the wave vector does not approach the commensurate value at low temperature. [S. Girault, A. H. Moudden, J. P. Pouget, and J. M. Godard, Phys. Rev. B **38**, 7980 (1988)].
[36]Comparing notations of Refs. 28 and 34, Mo(3)=Mo I and Mo(2)=Mo II.